

Available online at www.sciencedirect.com

ScienceDirect

www.elsevier.com/locate/jes

JES
 JOURNAL OF
 ENVIRONMENTAL
 SCIENCES
www.jesc.ac.cn

Mercury photoreduction and photooxidation in lakes: Effects of filtration and dissolved organic carbon concentration

Nelson J. O'Driscoll^{1,*}, Emma Vost¹, Erin Mann¹, Sara Klapstein¹, Robert Tordon², Matthew Lukeman³

1. Department of Earth & Environmental Science, Acadia University, Wolfville B4P 2R6, Nova Scotia, Canada

2. Environment Canada, Dartmouth, Nova Scotia, Canada

3. Department of Chemistry, Acadia University, Wolfville B4P 2R6, Nova Scotia, Canada

ARTICLE INFO

Article history:

Received 29 June 2017

Revised 27 November 2017

Accepted 6 December 2017

Available online 22 December 2017

Keywords:

Mercury

Photoreduction

Photooxidation

Dissolved organic carbon (DOC)

Particulates

Kejimikujik National Park

ABSTRACT

Mercury is a globally distributed, environmental contaminant. Quantifying the retention and loss of mercury is integral for predicting mercury-sensitive ecosystems. There is little information on how dissolved organic carbon (DOC) concentrations and particulates affect mercury photoreaction kinetics in freshwater lakes. To address this knowledge gap, samples were collected from ten lakes in Kejimikujik National Park, Nova Scotia (DOC: 2.6–15.4 mg/L). Filtered (0.2 μ m) and unfiltered samples were analysed for gross photoreduction, gross photooxidation, and net reduction rates of mercury using pseudo first-order curves. Unfiltered samples had higher concentrations ($p = 0.04$) of photoreducible divalent mercury ($\text{Hg(II)}_{\text{RED}}$) (mean of 754 ± 253 pg/L) than filtered samples (mean of 482 ± 206 pg/L); however, gross photoreduction and photooxidation rate constants were not significantly different in filtered or unfiltered samples in early summer. DOC was not significantly related to gross photoreduction rate constants in filtered ($R^2 = 0.43$; $p = 0.08$) and unfiltered ($R^2 = 0.02$; $p = 0.71$) samples; DOC was also not significantly related to gross photooxidation rate constants in filtered or unfiltered samples. However, DOC was significantly negatively related with $\text{Hg(II)}_{\text{RED}}$ in unfiltered ($R^2 = 0.53$; $p = 0.04$), but not in filtered samples ($R^2 = 0.04$; $p = 0.60$). These trends indicate that DOC is a factor in determining dissolved mercury photoreduction rates and particles partially control available $\text{Hg(II)}_{\text{RED}}$ in lake water. This research also demonstrates that within these lakes gross photoreduction and photooxidation processes are close to being in balance. Changes to catchment inputs of particulate matter and DOC may alter mercury retention in these lakes and could partially explain observed increases of mercury accumulation in biota.

© 2017 The Research Center for Eco-Environmental Sciences, Chinese Academy of Sciences.

Published by Elsevier B.V.

Introduction

Mercury is a toxic metal that is present in the environment in several forms. Elemental mercury (Hg(0)) is highly volatile, and

is the dominant form in the atmosphere due to its low solubility in water and high vapour pressure. Divalent mercury (Hg(II)) is highly soluble and is the primary form deposited to freshwater ecosystems. Once in these ecosystems, Hg(II) can readily bind to

* Corresponding author. E-mail: nelson.odriscoll@acadiau.ca (Nelson J. O'Driscoll).

particles and dissolved ligands (such as dissolved organic matter (DOM)) in lake water (Allard and Arsenie, 1991; Garcia et al., 2005a; Xiao et al., 1995). Some of the available Hg(II) in a lake may be subsequently converted to organic mercury compounds, primarily methyl mercury ($\text{CH}_3\text{Hg(I)}$) which can bioaccumulate in food webs and cause neurotoxic effects in upper trophic level organisms (Schroeder and Munthe, 1998).

Dissolved gaseous mercury (DGM) is thought to be primarily comprised of Hg(0) formed from *in situ* Hg(II) reduction reactions (O'Driscoll et al., 2004; Schroeder and Munthe, 1998). DGM can volatilise from water to air and thus be removed from aquatic ecosystems (Fig. 1; O'Driscoll et al., 2005). Some studies have shown that DGM volatilisation can equal the mass of mercury input from wet deposition in many freshwater systems (Amyot et al., 1994; O'Driscoll et al., 2005), and volatilisation from the world's oceans may account for approximately 30% of total global mercury emissions to the atmosphere (Mason et al., 1994). Although several mercury cycling models, such as the Regional Mercury Cycling Model (Harris et al., 1996), have been produced, there are still large sources of error in the mercury flux values produced by these models, particularly when comparing between ecosystems (Schroeder and Munthe, 1998). One reason for the large errors in mercury flux values may be that the specific processes and fundamental reaction rates governing mercury photoreduction and photooxidation have neither been quantified, nor related to lakewater characteristics (Lalonde et al., 2001).

Atmospheric mercury is globally distributed and can be deposited through rainfall and other deposition processes to remote ecosystems with no point sources (Fitzgerald et al., 1998; O'Driscoll et al., 2005). While deposition patterns vary, there is no clear explanation as to why some remote lakes have elevated levels of mercury while other similar lakes do not (Lavoie et al., 2013). Research by the METAALICUS mercury research network and others has shown that substantial amounts of Hg(II) deposited to lakes are quickly reduced to Hg(0) by solar radiation-driven reactions, and this volatilises back to the atmosphere (38%–59% after eight weeks) (Amyot et al., 1997; Orihel et al., 2007). Orihel et al. (2007) also suggest that the remaining mercury that is not volatilised is more efficiently incorporated into the food web than previously-present mercury; however, recent work by Luo et al. (2017) found that with time, the reactivity and bioavailability of mercury deposited to aquatic environments may decrease, potentially through the formation of mercury (II) sulphide (HgS) by photoreactions of mercury and DOM. Therefore, the higher the efficiency of photoreduction, and the greater the time elapsed since deposition, the less likely it is that mercury will be retained in a lake and subsequently methylated to the bioaccumulative form. We know from previous work that ultraviolet (UV) radiation (280–400 nm) is key to both photoreduction and photooxidation reactions of mercury in freshwater systems (Amyot et al., 1994; O'Driscoll et al., 2006).

The lakes in Kejimikujik National Park (KNP), Nova Scotia, Canada are an especially suitable system for this study not only

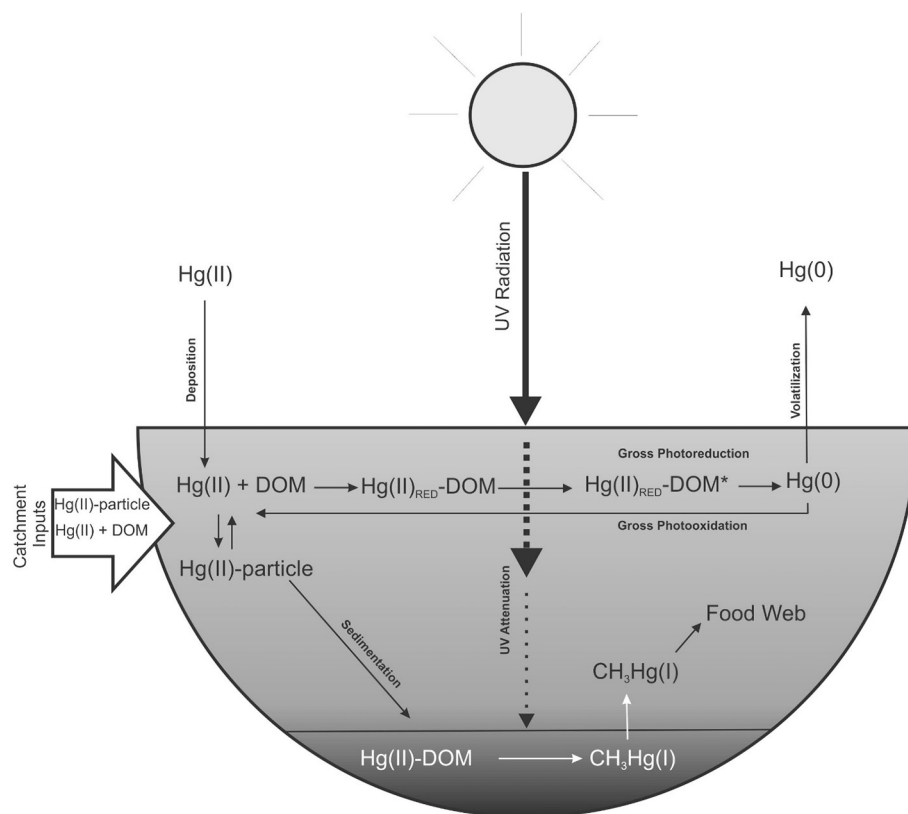


Fig. 1 – Conceptual diagram showing relationships between mercury gross photoreduction, gross photooxidation, photoreducible divalent mercury ($\text{Hg(II)}_{\text{RED}}$), dissolved organic matter (DOM) and particles in a typical freshwater lake. Intramolecular DOM facilitated mercury photoreaction is proposed (adapted from Vost et al. (2012)).

because of their history of elevated mercury contamination (Wyn et al., 2010), but also because of their wide variability in DOM concentrations within a small geographic area (Harris et al., 2002). Many lakes in KNP are on low-lying topography, which results in some lakes having large wetland areas in their catchments, high dissolved organic carbon (DOC), and DOC-associated mercury levels (Meng et al., 2005; Ravichandran, 2004).

Dissolved organic matter (primarily measured as DOC) can influence a watershed's ability to retain or volatilise mercury, since DOC is known to be a key ligand for many forms of mercury in freshwaters (O'Driscoll et al., 2004; United States Environmental Protection Agency, 2002). However, the relationship between DOC and mercury photoreactions is still poorly constrained, as it is unclear whether mercury's association with DOC enhances or inhibits mercury photoreactions. Amyot et al. (1994) found that lakes with higher DOC concentrations had lower Hg(0) production, and Tseng et al. (2004) found that DOC plays a significant role in inhibiting the formation of DGM in Alaskan lakes, suggesting that increased DOC either inhibits radiation penetration, or complexes mercury in a way that makes it unavailable for photoreduction. Other studies have suggested that mercury evasion rates are independent of DOC concentrations (Amyot et al., 1997; Wollenberg and Peters, 2009), and Amyot et al. (1997) determined that DGM production was not influenced by the amount of available DOC in high Arctic lakes. Yet other studies (Boudala et al., 2000; O'Driscoll et al., 2004; Xiao et al., 1995), point to a positive relationship between Hg(0) photoproduction and DOC. In lakes, where it is believed that DOC is the ultimate electron donor in the Hg(II) reduction mechanism, and the DOC-bound mercury may be highly photosensitive (Jeremiason et al., 2015). Another confounding variable in determining the DOC effect on mercury photoreactions is the presence of particulate material in freshwaters, which may bind both Hg(II) and Hg(0) forms, altering the amount available for photoreactions; Wang et al. (2015) found that up to 70% of the Hg(0) in freshwater may be bound to particulate matter and unavailable for photoreactions. It is currently unknown to what extent photoreducible Hg(II) is affected by the presence of particulate matter.

Knowing the concentration of DOC and levels of photo-reducible Hg(II) in the water column are important factors for determining the rate of DGM production, yet most previous flux studies have been field-based, making it difficult to determine which factors have the most influence on mercury photoreduction. It is recognised that net photoproduction of Hg(0) is a result of the balance between photoreduction and photooxidation in a system; however, gross photoreduction and photooxidation rate constants for mercury in a series of lakes have not yet been quantified, and the role of filtration on these processes is currently unknown. Wang et al. (2015) recently concluded that particulate-bound Hg(0) may comprise up to 70% of the elemental mercury in natural waters, and that this fraction was non-purgeable; however, the interactions between particulates, microbiology, and photochemical reactions are still unclear. As such, we are presently unable to distinguish the fundamental photochemical characteristics that partially control mercury accumulation or loss in lakes.

The aim of this research was to quantify gross photoreduction, gross photooxidation, and net photoreduction rates of mercury for both filtered and unfiltered water from a series of

lakes in Kejimikujik National Park, Nova Scotia, with a range of DOC concentrations. Using this data, we examined the influence of DOC and particulates on mercury photochemical rate constants and the amount of photoreducible Hg(II). These fundamental kinetic results are critical to future predictive modelling, as an important tool for identifying and managing freshwaters that retain mercury, and are therefore mercury-sensitive ecosystems susceptible to mercury contamination.

1. Methods

1.1. Sampling and experimental preparation

Ten lakes (Big Dam East, Big Dam West, North Cranberry, Grafton, Puzzle, Big Red, Mountain, Beaverskin, Peskowsk, and Pebbleloggitch) were sampled in May of 2009, or in August of 2010 (Appendix A Fig. SI-1). Big Dam East and Big Dam West Lakes were also sampled in May of 2008 however Big Dam East 2008 summary data was not available for this paper. Lakes were chosen to provide a wide range of DOC concentrations (1.5 to 14.2 mg/L). Surface water was sampled from the middle of each lake using a canoe, or from another representative site within the lake. Water was collected in pre-cleaned 24 L HDPE containers by hand just below the lake surface, using clean powder free gloves. Containers were filled approximately $\frac{3}{4}$ full, and frozen at -20°C in the dark until analysis.

Water samples were thawed overnight at room temperature before analysis, and then were kept at 25°C for the duration of the analysis. For the filtered treatment, vacuum filtration with $0.2\ \mu\text{m}$ Teflon filters was performed, where residual organic carbon was removed from Teflon filters before use by washing each with 200 mL of organic carbon-free DI water. This filtration technique has been shown to result in minimal microbial activity for >8 hr in freshwater samples (Lean and Siciliano, 2003). Before and after irradiation, water samples were sub-sampled in triplicate for total mercury (THg) analysis, using trace clean 40 mL glass vials with Teflon caps, preserved with 1% BrCl, and then stored in the dark at 4°C . Subsamples were also taken for DOC and dissolved inorganic carbon (DIC) analysis, using 50 mL polypropylene tubes, and frozen until analysis. Anion and cation samples were taken using 50 mL polypropylene tubes; anion samples were frozen until analysis and cation samples were preserved with 1% OMNI-trace nitric acid.

Before use, all apparatus (300 mL sparger, silicone stoppers, Teflon tubes, vacuum filtration apparatus) were autoclaved at 135°C for 20 min, placed in a 20% HCl acid bath overnight, and then triple rinsed with Milli-Q deionized (DI) water. The system (Appendix A Fig. SI-2) was then blanked for mercury by irradiating with high intensity UV radiation (five UVA and five UVB bulbs; see Appendix A Fig. SI-3) with mercury-free zero air pumped through the system until Hg(0) readings were less than $0.01\ \text{ng}/\text{m}^3$ (instrumental detection limit), as measured by a Tekran model 2537B cold vapour atomic fluorescence automated mercury analyser.

1.2. Irradiation system and gross reduction analysis

The analysis system (Appendix A Fig. SI-2) consisted of a $300\ \text{cm}^3$ quartz sparger (6 cm in diameter, 9.6 cm in height,

with a platinum cured silicone stopper and Teflon tubes for air flow) placed inside a LuzChem ORG photoreactor maintained at a constant temperature of $25 \pm 1^\circ\text{C}$. Prior to irradiation, mercury-free zero air from a Tekran model 1100 was bubbled through the 200 mL sample at 1 L/min, in the dark, until readings were less than the Tekran model 2537B instrumental detection limit ($<0.1 \text{ ng/m}^3$), removing any existing DGM present prior to irradiation, and “blanking” the samples. Blanked samples (filtered and unfiltered) were then irradiated using one UVA and one UVB bulb in the LuzChem, following the methods of Qureshi et al. (2010) and O’Driscoll et al. (2004), while continuously bubbling with zero air and quantifying gaseous Hg(0) production with the Tekran 2537B. By continuously bubbling the sample at 1 L/min DGM was purged as it was formed in the quartz sparger (Appendix A Fig. SI-2), and so the mercury oxidation/reduction equilibrium was pushed primarily towards reduction, as outlined by O’Driscoll et al. (2006). The integrated spectral intensity applied to samples by the LuzChem, for the 280–400 nm range, was quantified to be 0.216 W/m^2 inside the quartz sparger, using an Ocean Optics USB 4000 spectroradiometer with a 10 m fibre optic probe. In the UV portion of the spectrum, these lamps approximate standard solar radiation at Earth’s surface (Appendix A Fig. SI-3). Irradiation of samples continued for approximately 20 hr, or until purged Hg(0) concentrations were consistently below the analytical detection limit ($<0.1 \text{ ng/m}^3$).

The ~20 hr continuous mercury concentration data, collected for a gross mercury reduction analysis curve, was corrected using the mean of ten readings taken following irradiation, when Hg(0) concentrations were consistently below detection limits of the instrument (0.1 ng/m^3). Corrected mercury concentrations were plotted cumulatively, and as such the graph approaches a maximum, which represents the total available photoreducible mercury in the lake water sample (Fig. 2). The pseudo first-order reduction rate constant (k value) was derived using a pseudo first-order kinetics equation (O’Driscoll et al., 2006), and fitting the integrated solution to the experimental data (see Eqs. (1), (2) and (3)) using SigmaPlot 12.0.

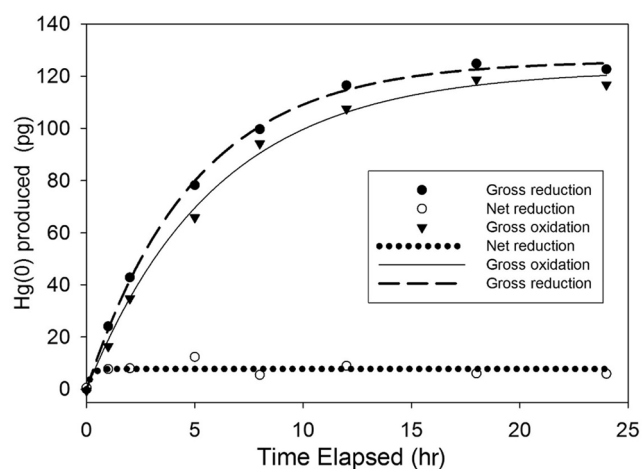


Fig. 2 – Gross photoreduction, gross photooxidation, and net photoreduction data and pseudo first-order fitted curves for 200 mL of filtered (abiotic) North Cranberry Lake water, sampled in May 2009.

The derivative for a first-order reaction showing loss of reducible mercury is:

$$d[\text{Hg(II)}_{\text{RED}}]/dt = -k[\text{Hg(II)}_{\text{RED}}]_0 \quad (1)$$

where: $d[\text{Hg(II)}_{\text{RED}}]/dt$ is the change in photoreducible mercury with time, and $[\text{Hg(II)}_{\text{RED}}]_0$ is the total amount of photoreducible mercury available in solution. The integrated form of this equation for a cumulative plot of the photoreduction product, DGM, or Hg(0) in solution, is:

$$\text{Hg(0)}_t = [\text{Hg(II)}_{\text{RED}}]_0 - e^{-kt}[\text{Hg(II)}_{\text{RED}}]_0 \quad (2)$$

This can be rewritten as:

$$\text{Hg(0)}_t = [\text{Hg(II)}_{\text{RED}}]_0 (1 - e^{-kt}) \quad (3)$$

where: Hg(0)_t (pg) is the mass of cumulative Hg(0), or DGM, removed from solution at any time t (hr), $[\text{Hg(II)}_{\text{RED}}]_0$ (pg) is the total mass of photoreducible mercury initially available in solution (equal to the final amount of cumulative Hg(0) produced), k (hr^{-1}) is the photoreduction rate constant (hr^{-1}), and t (hr) is elapsed time (hr).

1.3. Net mercury photoreduction and photooxidation

To analyse net reduction rates, 270 mL of lake water (filtered or unfiltered) was decanted into 9 pre-cleaned (sterilized, acid washed and pre-irradiated) quartz glass beakers, and sealed with silicone caps such that no air was present, preventing loss of DGM to the headspace. A zero-hour sample was analysed for Hg(0) immediately, and sub-sampled for other analyses. Samples were irradiated and analysed for Hg(0) at 1, 2, 5, 8, 12, 18 and 24 hr, and a 24 hr dark control was prepared and analysed. Prior to analysis, 70 mL of the sample was discarded, and the remaining 200 mL was bubbled to quantify DGM using a Tekran 2537B, similar to Qureshi et al. (2010).

The net reduction kinetic results were derived using the same curve fitting technique for Hg(0) produced vs. time, as described above for gross photoreduction. Once the gross reduction and net reduction rate constants were determined, gross photooxidation rate constants were derived by subtracting net photoreduction data points from gross photoreduction data, and a pseudo first-order reaction equation was fitted to the resulting curve using SigmaPlot 12.0 (Fig. 2). Differences between groups were tested by t -test with the Shapiro–Wilk normality testing.

1.4. Total mercury and dissolved organic carbon, anion, and cation analyses

Non-irradiated water was sampled for total mercury (THg; in triplicate), for dissolved carbon (DOC/DIC), and for easily reducible mercury. Total mercury was quantified in samples following United States Environmental Protection Agency (US EPA) Method 1631 (United States Environmental Protection Agency, 2002), using gold amalgamation cold vapour atomic fluorescence spectroscopy with a Tekran model 2600. DOC analysis was performed in triplicate using a Shimadzu TOC-V/TOC-CPN with ASI-V auto-sampler analyser, which uses thermal decomposition and wet oxidation, with CO_2 detection by infrared spectroscopy, to determine total carbon and

inorganic carbon (organic carbon measured by difference). DOC and anion samples were preserved by freezing in polypropylene containers, with storage at -20°C and cation samples preserved with 1% OMNI-trace nitric acid. Analysis for sodium, magnesium, potassium, calcium, manganese, zinc, barium, and iron was performed at Acadia University using inductively coupled plasma-mass spectrometry (ICP-MS; Perkin Elmer SCIEX ELAN DRC-e Inductively Coupled Plasma-Mass Spectrometer) with a dynamic reaction cell (DRC) to reduce mass interferences. Anions (chlorine and sulphate) were quantified using a Metrohm ion chromatograph.

2. Results and discussion

2.1. Total photoreducible mercury

An integrated pseudo first-order reaction model was found to fit all the gross mercury photoreduction data well ($R^2 > 0.98$; $p < 0.0001$; e.g. Fig. 2, Appendix A Fig. SI-4). In all lakes, unfiltered samples had significantly higher concentrations of photoreducible mercury, $\text{Hg(II)}_{\text{RED}}$ (mean = 754 ± 253 pg/L) than $0.2 \mu\text{m}$ filtered samples (mean = 482 ± 206 pg/L) (t-test; $p = 0.04$; Shapiro-Wilk normality $p = 0.63$). This indicates that some $\text{Hg(II)}_{\text{RED}}$ was lost during the filtration process, either due to the association of these mercury species with particles, or binding to the filtration apparatus. This difference in filtered vs. non-filtered $\text{Hg(II)}_{\text{RED}}$ may also indicate that bacteria and microorganisms such as algae and phytoplankton play a role in mercury photoreduction, since $0.2 \mu\text{m}$ filtration will remove these organisms; however, it is not clear if these organisms access the same pool of reducible mercury as abiotic photoreactions (Baeyens and Leermakers, 1998; Deng et al., 2008; Siciliano et al., 2002). It is further possible that microbes may convert some of the mercury on particles into photoreducible mercury ($\text{Hg(II)}_{\text{RED}}$), similar to the mechanism proposed by Pannu et al. (2014) in soils.

2.2. Gross mercury photoreduction and photooxidation

In this work, gross photoreduction rate constants ranged from 1.63×10^{-3} to $3.42 \times 10^{-3}\text{hr}^{-1}$ in filtered samples, and 1.29×10^{-3} to $2.93 \times 10^{-3}\text{hr}^{-1}$ in unfiltered samples, for lakes sampled in May of 2008 and 2009 (Table 1). Similar results were found for the gross photooxidation rate constants, which ranged between 1.42×10^{-3} and $3.04 \times 10^{-3}\text{hr}^{-1}$ for filtered samples, and 1.21×10^{-3} and $2.78 \times 10^{-3}\text{hr}^{-1}$ for unfiltered samples (Table 1). It can be seen in Table 1 that the lakes sampled late in the summer season (August of 2010; Pebbleogitch, Peskowsk, and Beaverskin lakes) have significantly larger gross photoreduction and gross photooxidation rate constants than the lakes sampled in early summer (Table 1). It is interesting to note, however, that the net photoreduction rate constants are in a similar range for all lakes; this suggests that while the rate of both photooxidation and photoreduction reactions has increased, the overall effect on the net mercury reduction rate constant did not change substantially, due to the close balance of photoreduction and photooxidation reactions occurring in these lakes. The

near-balance of mercury photooxidation and photoreduction observed in these lakes may suggest a common linking component between lakes, such as the atmospheric deposition of reactive mercury being the dominant mercury pool undergoing these photoreactions (Orihel et al., 2007).

Our data show that gross photoreduction (mean = $2.46 \times 10^{-3}\text{hr}^{-1}$, standard deviation (SD) = $6.72 \times 10^{-4}\text{hr}^{-1}$ for filtered; mean = $2.07 \times 10^{-3}\text{hr}^{-1}$, SD = $5.08 \times 10^{-4}\text{hr}^{-1}$ for unfiltered) and photooxidation rate constants (mean = $2.04 \times 10^{-3}\text{hr}^{-1}$, SD = $5.57 \times 10^{-4}\text{hr}^{-1}$ for filtered; mean = $2.00 \times 10^{-3}\text{hr}^{-1}$, SD = $4.76 \times 10^{-4}\text{hr}^{-1}$ for unfiltered) are not significantly different between filtered and unfiltered lake waters, sampled in early summer (respective t-tests; $p = 0.2$; $p = 0.8$); this demonstrates that the rate constants of these mercury photoreactions are not significantly affected by the presence of particles or particle-bound mercury species in solution. This result is in contrast to the results for photoreducible mercury amounts ($\text{Hg(II)}_{\text{RED}}$) presented above, which do show significant differences between filtered and unfiltered samples. This lack of an effect on rate constants by the presence or absence of $0.2 \mu\text{m}$ filterable material supports the conclusions of Qureshi et al. (2010) and Beucher et al. (2002), who observed no substantial influence of filtration (or biotic activity) on mercury reduction rate constants in ocean water. Relative standard error associated with the derivation of the rate constant for gross photoreduction was $<1\%$ in all cases and was higher for gross photooxidation ($<10\%$ in all cases except 34% for BDE). The higher error on the gross photooxidation results is a result of the higher error associated with net photoreduction experiments due to the low masses of mercury being quantified. There is very limited data available in the literature for mercury photooxidation rate constants. Lalonde et al. (2001) found the net mercury photooxidation rate constant for a freshwater river was $0.26/\text{hr}$ which is lower but not a good point of comparison for the gross photooxidation rates measured here. Our results are more comparable to the work of Garcia et al. (2005b) who calculated gross mercury photooxidation rate constants for freshwaters ranging from 0.02 to 0.07hr^{-1} .

2.3. Net mercury photoreduction

Rate constants for net photoreduction were derived similarly using a method analogous to that used for the gross photoreduction determinations, and assuming pseudo first-order rate kinetics using Eq. (3) (Table 1, Appendix A Fig. SI-5). The fit was not as strong for these experiments (R^2 values ranging 0.22 to 0.91, p -values ranging 0.0003–0.25), which may be a result of the Hg(0) levels close to the method detection limit being produced at each 5-minute sampling period, and therefore being subject to greater error. The mean concentration of net Hg(0) (i.e. DGM) measured in water from all lakes was approximately 8.5% of the total $\text{Hg(II)}_{\text{RED}}$ for the gross photoreduction experiments (ranging 15 to 80 pg/L; mean = 41 ± 17.5 pg/L). This result indicates that there is a much larger capacity for mercury photoreduction and volatilisation from these lakes that might be released with decreases in gross photooxidation kinetics. The net mercury reduction rate constants derived from the data for filtered samples (ranging 1.28×10^{-5} to $8.30 \times 10^{-1}\text{hr}^{-1}$; mean = $1.15 \times 10^{-1}\text{hr}^{-1}$; SD = $2.71 \times 10^{-1}\text{hr}^{-1}$) and for unfiltered samples (ranging 3.20×10^{-1} to $1.93 \times 10^0\text{hr}^{-1}$; mean = $8.77 \times 10^{-1}\text{hr}^{-1}$;

Table 1 – Rate constants (k ; hr^{-1}) derived for gross photoreduction, net photoreduction, and gross photooxidation of mercury with standard error from curve fitting technique and total photoreducible divalent mercury ($\text{Hg(II)}_{\text{RED}}$; pg/L). Note that lakes sampled in August 2010 are highlighted in grey, lakes sampled in May of 2008 and 2009 are not highlighted.

0.2 um Filtered Samples							
Lake	Gross Photoreduction k (h^{-1})	Standard Error	$\text{Hg(II)}_{\text{RED}}$ (pg L^{-1})	Net Photoreduction k (h^{-1})	Standard Error	Gross Photooxidation k (h^{-1})	Standard Error
Big Dam East (2009)	3.27E-03	1.64E-05	270	7.30E-01	1.28E+01	1.64E-03	5.58E-04
Big Dam West (2008)	2.19E-03	7.71E-06	475	5.05E-01	2.41E-01	1.98E-03	6.70E-05
Big Dam West (2009)	1.63E-03	6.80E-06	690	4.53E-01	3.10E-01	1.42E-03	6.62E-05
North Cranberry (2009)	2.46E-03	1.58E-05	615	4.56E+00	2.33E+01	2.17E-03	1.37E-04
Grafton (2009)	1.81E-03	1.46E-05	840	1.04E+00	3.46E-01	1.61E-03	1.20E-04
Puzzle (2009)	3.13E-03	5.39E-06	455	1.51E+00	1.91E+00	2.82E-03	7.02E-05
Big Red (2009)	1.81E-03	1.13E-05	240	1.28E-05	7.55E-02	1.67E-03	1.49E-04
Mountain (2009)	3.42E-03	2.22E-05	270	8.30E+01	4.58E-01	3.04E-03	1.51E-04
Beaverskin (2010)	8.15E-01	5.40E-03	NA	1.81E-01	1.36E+00	4.76E-06	3.86E-02
Peskowesk (2010)	3.07E-01	1.70E-03	NA	6.43E-01	2.57E-01	5.34E-06	7.80E-03
Pebblelogitch (2010)	8.16E-02	4.00E-04	NA	4.36E-01	2.76E-01	9.58E-02	1.83E-02
Unfiltered Samples							
Lake	Gross Photoreduction k (h^{-1})	Standard Error	$\text{Hg(II)}_{\text{RED}}$ (pg L^{-1})	Net Photoreduction k (h^{-1})	Standard Error	Gross Photooxidation k (h^{-1})	Standard Error
Big Dam East (2009)	2.20E-03	1.13E-05	795	1.04E+00	8.63E-01	1.90E-03	8.36E-05
Big Dam West (2008)	1.63E-03	9.69E-06	835	5.03E-01	2.73E-01	1.53E-03	7.10E-05
Big Dam West (2009)	1.29E-03	1.51E-05	700	6.19E-01	2.89E-01	1.21E-03	9.15E-05
North Cranberry (2009)	2.16E-03	3.93E-06	975	7.80E-01	1.42E+00	1.79E-03	1.37E-04
Grafton (2009)	1.56E-03	4.81E-06	995	5.31E-01	5.14E-01	2.08E-03	2.55E-04
Puzzle (2009)	2.39E-03	7.52E-06	1005	1.30E+00	1.05E+00	2.24E-03	5.09E-05
Big Red (2009)	2.43E-03	1.71E-05	255	3.20E-01	1.05E-01	2.50E-03	1.24E-04
Mountain (2009)	2.93E-03	9.69E-06	470	1.93E+00	2.44E+00	2.78E-03	9.73E-05
Beaverskin (2010)	3.39E-01	2.35E-02	NA	1.05E+00	6.85E-01	2.06E-01	8.90E-03
Peskowesk (2010)	1.64E-01	8.00E-04	NA	7.62E-01	2.89E-01	4.89E-02	3.70E-03
Pebblelogitch (2010)	1.12E-01	4.00E-04	NA	5.31E-01	5.14E-01	5.41E-02	2.40E-02

$\text{SD} = 4.96 \times 10^{-1} \text{hr}^{-1}$) were more variable than those derived from the gross photoreduction experiments (Table 1). Many studies have focussed on the *in situ* net photoreduction of mercury in aquatic systems; for example, Poulain et al. (2004) determined that the DGM formation rate constant ranged from 0.76 to 1.4hr^{-1} in a wetland area, and 0.21 to 0.47hr^{-1} for a pelagic area. Another study by Amyot et al. (1994) determined the mean net mercury reduction rate constant to be 0.10/hr. A review by Vost et al. (2012) found that net mercury reduction rate constants ranged between 0.1 and 2.2/hr for freshwater samples, which are within the range of net mercury photoreduction constants measured in this study for unfiltered water samples. However, the unfiltered water samples show slower rates possibly due to slow release of reducible mercury from solid particles in unfiltered samples similar to what has been proposed between soil particles and soil solution (Pannu et al., 2014).

2.4. Relationship of DOC and particulates with rate constants and $\text{Hg(II)}_{\text{RED}}$

Dissolved organic carbon, as well as major cations and anions spanned a wide range in the lakes sampled (Appendix A Table SI-1). Minimal variation was observed between pre- and post-irradiation DOC concentration in samples (mean difference < 10%). These small variations were within acceptable error, and could be a result of DOC mineralization or small

amounts of bacterial growth in the apparatus over the 24-hour period.

DOC was plotted against the gross photoreduction and gross photooxidation rate constants for filtered and unfiltered lakes, and also against $\text{Hg(II)}_{\text{RED}}$ (Fig. 3A, B, C). Gross photooxidation rate constants were not significantly related to DOC in filtered ($R^2 = 0.20$, $p > 0.10$) or unfiltered samples ($R^2 = 0.0007$; $p > 0.10$). There was no significant linear relationship between DOC and the gross photoreduction rate constants in either filtered ($R^2 = 0.43$; $p = 0.08$) or unfiltered ($R^2 = 0.02$; $p = 0.71$) samples (Fig. 3B). While not statistically significant, the trend suggests that in filtered water samples, as DOC increases, the rate at which photoreducible mercury is converted to Hg(0) may slow; this slowing of mercury photoreduction with increasing DOC in filtered water agrees with findings of a study done by Garcia et al. (2005a), who examined DOC fluorescence and DGM, finding that DGM was negatively correlated with DOC. However more data is required to determine if this trend is significant in larger numbers of samples. In the unfiltered samples it is possible that particulate-bound Hg(II) and Hg(0) that are variable with respect to biological transformations and photoreactivity interfere with this relationship and so a much weaker interaction is observed.

In contrast to the lack of significant relationships between DOC and photoreduction rate constants, there is a significant negative linear relationship ($R^2 = 0.53$; $p = 0.04$) between DOC and $\text{Hg(II)}_{\text{RED}}$ observed in unfiltered samples, and no

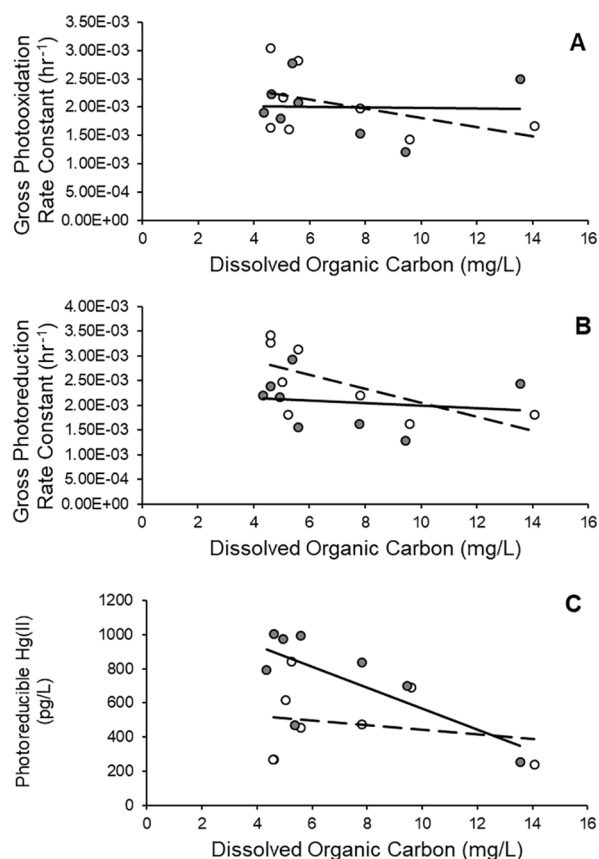


Fig. 3 – Dissolved organic carbon (DOC; mg/L) plotted against (A) the gross photooxidation rate constant (hr^{-1} ; filtered $R^2 = 0.20$, $p > 0.10$ and unfiltered $R^2 < 0.01$, $p > 0.10$), (B) the gross photoreduction rate constant (hr^{-1} ; filtered $R^2 = 0.43$, $p = 0.08$ and unfiltered $R^2 = 0.02$, $p = 0.71$), and (C) photoreducible divalent mercury (Hg(II) ; pg/L; filtered $R^2 = 0.04$, $p = 0.60$ and unfiltered $R^2 = 0.53$, $p = 0.04$) for both filtered (open circles) and unfiltered samples (shaded circles), respectively, from 7 lakes in Kejimikujik National Park (lakes sampled in 2008 and 2009). No significant relationship was observed with photooxidation rate constants. Lakes sampled in August 2010 have substantially larger gross photoreduction rate constants (see Table 1) and are excluded from this graph.

relationship ($R^2 = 0.04$; $p = 0.64$) observed in filtered samples (Fig. 3C). This result suggests that particulate-bound species of mercury are likely driving the availability of $\text{Hg(II)}_{\text{RED}}$ in these freshwaters, and this is linked to the availability of DOC in solution. It is possible that the formation of flocculated dissolved organic matter into particulate organic matter in solution is the explanation for this relationship, which suggests that much more information on the seasonal dynamics of this particulate fraction and the availability of $\text{Hg(II)}_{\text{RED}}$ is required. Due to the tight association between gross photoreduction and gross photooxidation rate constants, similar relationships are observed between DOC and gross photooxidation rate constants for filtered and unfiltered lake samples.

Mercury photoreduction in lakes has been suggested to be a key process regulating newly deposited reactive mercury in freshwaters (Orihel et al., 2007). Luo et al. (2017) also suggested that photoreactions might limit the availability of this

reactive mercury to be methylated. As such, photoreactions may be critical to regulating mercury uptake in food webs. Our data supports the notion that both DOC and particulate organic matter play important role in determining the kinetics of mercury photoreduction in lake water. While the role of DOC has been suggested by numerous studies (Allard and Arsenie, 1991; Amyot et al., 1994, 1997; Garcia et al., 2005a; Mason et al., 1994), the importance of particulate matter has only recently become clear (Wang et al., 2015). A major finding of this study is that gross photooxidation and gross photoreduction rates are close to being in balance for the sampled lakes of Kejimikujik National Park, in the summer. In addition, DOC and particulate matter are important characteristics controlling the rate of mercury photoreduction and the availability of photoreducible divalent mercury ($\text{Hg(II)}_{\text{RED}}$). It should be noted that a more detailed model of mercury photoreactions among natural water ecosystems would also need to include changes in dissolved ions as a predictive factor affecting interactions with DOC and particles. As such, any future changes in DOM and particulate content from catchment inputs may significantly affect mercury photoreactions, and therefore the balance of mercury retention versus loss in these lake ecosystems (Fig. 1). This research may, in part, help to explain temporal changes in mercury retention in this location and ultimately the relatively high and increasing levels of mercury found in biota of Kejimikujik (Evers et al., 2007; Little et al., 2015; Wyn et al., 2010). Future research should focus on seasonal and multiannual changes in photoreducible mercury and particulate matter to see if this is a plausible hypothesis for the mercury retention observed in this freshwater ecosystem.

Acknowledgments

This project was funded by NSERC (CGS-M scholarship to E.V. and discovery grant (Grant# 341960-2013) to N.O.), the Canada Research Chairs Program (Grant# 950-203477 to N.O.), and the Canada Foundation for Innovation (Grant# 203477 to N.O.). Thanks also to the staff of the K.C. Irving Environmental Science Centre and technical support from Environment Canada.

Appendix A. Supplementary data

Supplementary data to this article can be found online at <https://doi.org/10.1016/j.jes.2017.12.010>.

REFERENCES

- Allard, B., Arsenie, I., 1991. Abiotic reduction of mercury by humic substances in aquatic system — an important process for the mercury cycle. *Water Air Soil Pollut.* 56:457–464. <https://doi.org/10.1007/BF00342291>.
- Amyot, M., McQueen, D.J., Mierle, G., Lean, D.R.S., 1994. Sunlight-induced formation of dissolved gaseous mercury in lake waters. *Environ. Sci. Technol.* 28:2366–2371. <https://doi.org/10.1021/es00062a022>.

- Amyot, M., Lean, D., Mierle, G., 1997. Photochemical Formation of volatile mercury in high Arctic lakes. *Environ. Toxicol. Chem.* 16:2054–2063. <https://doi.org/10.1002/etc.5620161010>.
- Baeyens, W., Leermakers, M., 1998. Elemental mercury concentrations and formation rates in the Scheldt estuary and the North Sea. *Mar. Chem.* 60:257–266. [https://doi.org/10.1016/S0304-4203\(97\)00102-3](https://doi.org/10.1016/S0304-4203(97)00102-3).
- Beucher, C., Wong-Wah-Chung, P., Richard, C., Mailhot, G., Bolte, M., Cossa, D., 2002. Dissolved gaseous mercury formation under UV irradiation of unamended tropical waters from French Guyana. *Sci. Total Environ.* 290:131–138. [https://doi.org/10.1016/S0048-9697\(01\)01078-6](https://doi.org/10.1016/S0048-9697(01)01078-6).
- Boudala, F.S., Folkins, I., Beauchamp, S., Tordon, R., Neima, J., Johnson, B., 2000. Mercury flux measurements over air and water in Kejimikujik National Park, Nova Scotia. *Water Air Soil Pollut.* 122:183–202. <https://doi.org/10.1023/A:1005299411107>.
- Deng, L., Wu, F., Deng, N., Zuo, Y., 2008. Photoreduction of mercury(II) in the presence of algae, *Anabaena cylindrical*. *J. Photochem. Photobiol. B* 91:117–124. <https://doi.org/10.1016/j.jphotobiol.2008.02.005>.
- Evers, D.C., Han, Y.J., Driscoll, C.T., Kamman, N.C., Goodale, M.W., Lambert, K.F., et al., 2007. Biological mercury hotspots in the northeastern United States and southeastern Canada. *Bioscience* 57:29–43. <https://doi.org/10.1641/B570107>.
- Fitzgerald, W.F., Engstrom, D.R., Mason, R.P., Nater, E.A., 1998. The case for atmospheric mercury contamination in remote areas. *Environ. Sci. Technol.* 32:1–7. <https://doi.org/10.1021/es970284w>.
- Garcia, E., Amyot, M., Ariya, P.A., 2005a. Relationship between DOC photochemistry and mercury redox transformations in temperate lakes and wetlands. *Geochim. Cosmochim. Acta* 69:1917–1924. <https://doi.org/10.1016/j.gca.2004.10.026>.
- Garcia, E., Poulain, A.J., Amyot, M., Ariya, P.A., 2005b. Diel variations in photoinduced oxidation of Hg⁰ in freshwater. *Chemosphere* 59:977–981. <https://doi.org/10.1016/j.chemosphere.2004.09.107>.
- Harris, R., Gherini, S., Hudson, R.J.M., 1996. Regional Mercury Cycling Model (R-MCM): a model for mercury cycling in lakes. User's Guide and Technical Reference.
- Harris, R., Hutchinson, D., Radde, J., 2002. Mercury in Fish in Kejimikujik Park, Nova Scotia; Application of Regional Mercury Cycling Model to 24 Lakes. *Can. Wildl. Serv. Tetra Inc.*
- Jeremiason, J., Portner, J.C., Aiken, G., Tran, K.T., Dvorak, M.T., Hiranaka, A., et al., 2015. Photoreduction of Hg(II) and photodemethylation of methylmercury: the key role of thiol sites on dissolved organic matter. *Environ. Sci. Processes Impacts* <https://doi.org/10.1039/C5EM00305A>.
- Lalonde, J.D., Amyot, M., Kraepiel, A.M.L., Morel, F.M.M., 2001. Photooxidation of Hg(0) in artificial and natural waters. *Environ. Sci. Technol.* 35:1367–1372. <https://doi.org/10.1021/es001408z>.
- Lavoie, R.A., Jardine, T.D., Chumchal, M.M., Kidd, K.A., Campbell, L.M., 2013. Biomagnification of mercury in aquatic food webs: a worldwide meta-analysis. *Environ. Sci. Technol.* 47:13385–13394. <https://doi.org/10.1021/es403103t>.
- Lean, D.R.S., Siciliano, S., 2003. Production of methylmercury by solar radiation. *J. Phys. IV Proc.* 107:743–747. <https://doi.org/10.1051/jp4:20030408>.
- Little, M.E., Burgess, N.M., Broders, H.G., Campbell, L.M., 2015. Distribution of mercury in archived fur from little brown bats across Atlantic Canada. *Environ. Pollut.* 207:52–58. <https://doi.org/10.1016/j.envpol.2015.07.049>.
- Luo, H.W., Yin, X., Jubb, A.M., Chen, H., Lu, X., Zhang, W., et al., 2017. Photochemical reactions between mercury (Hg) and dissolved organic matter decrease Hg bioavailability and methylation. *Environ. Pollut.* 220 (Part B):1359–1365. <https://doi.org/10.1016/j.envpol.2016.10.099>.
- Mason, R.P., Fitzgerald, W.F., Morel, F.M.M., 1994. The biogeochemical cycling of elemental mercury: anthropogenic influences. *Geochim. Cosmochim. Acta* 58:3191–3198. [https://doi.org/10.1016/0016-7037\(94\)90046-9](https://doi.org/10.1016/0016-7037(94)90046-9).
- Meng, F.R., Arp, P., Sangster, A., Brun, G.L., Rencz, A.N., Hall, G., et al., 2005. Modeling dissolved organic carbon, total and methyl mercury in Kejimikujik freshwaters. *Mercury Cycling in a Wetland-dominated Ecosystem: A Multidisciplinary Study. Society of Environmental Toxicology and Chemistry (SETAC)*, pp. 1–19.
- O'Driscoll, N.J., Lean, D.R.S., Loseto, L.L., Carignan, R., Siciliano, S.D., 2004. Effect of dissolved organic carbon on the photoproduction of dissolved gaseous mercury in lakes: potential impacts of forestry. *Environ. Sci. Technol.* 38, 2664–2672.
- O'Driscoll, N.J., Rencz, A., Lean, D.R.S., 2005. The biogeochemistry and fate of mercury in the environment. *Met. Ions Biol. Syst.* 43, 221–238.
- O'Driscoll, N.J., Siciliano, S.D., Lean, D.R.S., Amyot, M., 2006. Gross photoreduction kinetics of mercury in temperate freshwater lakes and rivers: application to a general model of DGM dynamics. *Environ. Sci. Technol.* 40:837–843. <https://doi.org/10.1021/es051062y>.
- Orihel, D.M., Paterson, M.J., Blanchfield, P.J., Bodaly, R.A. (Drew), Hintelmann, H., 2007. Experimental evidence of a linear relationship between inorganic mercury loading and methylmercury accumulation by aquatic biota. *Environ. Sci. Technol.* 41:4952–4958. <https://doi.org/10.1021/es063061r>.
- Pannu, R., Siciliano, S.D., O'Driscoll, N.J., 2014. Quantifying the effects of soil temperature, moisture and sterilization on elemental mercury formation in boreal soils. *Environ. Pollut.* 193:138–146. <https://doi.org/10.1016/j.envpol.2014.06.023>.
- Poulain, A.J., Amyot, M., Findlay, D., Telor, S., Barkay, T., Hintelmann, H., 2004. Biological and photochemical production of dissolved gaseous mercury in a boreal lake. *Limnol. Oceanogr.* 49:2265–2275. <https://doi.org/10.4319/lo.2004.49.6.2265>.
- Qureshi, A., O'Driscoll, N.J., MacLeod, M., Neuhold, Y.-M., Hungerbühler, K., 2010. Photoreactions of mercury in surface ocean water: gross reaction kinetics and possible pathways. *Environ. Sci. Technol.* 44:644–649. <https://doi.org/10.1021/es9012728>.
- Ravichandran, M., 2004. Interactions between mercury and dissolved organic matter — a review. *Chemosphere* 55: 319–331. <https://doi.org/10.1016/j.chemosphere.2003.11.011>.
- Schroeder, W.H., Munthe, J., 1998. Atmospheric Mercury — An Overview. *Atmos. Environ., Atmospheric Transport, Chemistry and Deposition of Mercury* 32:pp. 809–822. [https://doi.org/10.1016/S1352-2310\(97\)00293-8](https://doi.org/10.1016/S1352-2310(97)00293-8).
- Siciliano, S.D., O'Driscoll, N., Lean, D.R.S., 2002. Dissolved gaseous mercury profiles in freshwaters. *Biogeochemistry of Environmentally Important Trace Element, ACS Symposium Series. American Chemical Society*:pp. 232–245 <https://doi.org/10.1021/bk-2003-0835.ch017>.
- Tseng, C.M., Lamborg, C., Fitzgerald, W.F., Engstrom, D.R., 2004. Cycling of dissolved elemental mercury in Arctic Alaskan lakes. *Geochim. Cosmochim. Acta* 68:1173–1184. <https://doi.org/10.1016/j.gca.2003.07.023>.
- United States Environmental Protection Agency, 2002. Method 1631, revision E: mercury in water by oxidation, purge and trap, and cold vapour atomic fluorescence spectrometry. EPA-821-R-02-01. U.S. EPA, Washington, D.C.
- Vost, E.E., Amyot, M., O'Driscoll, N.J., 2012. Photoreactions of mercury in aquatic systems. In: Liu, G., Cai, Y., O'Driscoll, N. (Eds.), *Environmental Chemistry and Toxicology of Mercury*. John Wiley & Sons, Inc., pp. 193–218.
- Wang, Y., Li, Y., Liu, G., Wang, D., Jiang, G., Cai, Y., 2015. Elemental mercury in natural waters: occurrence and determination of particulate Hg(0). *Environ. Sci. Technol.* 49:9742–9749. <https://doi.org/10.1021/acs.est.5b01940>.

- Wollenberg, J.L., Peters, S.C., 2009. Mercury emission from a temperate lake during autumn turnover. *Sci. Total Environ.* 407:2909–2918. <https://doi.org/10.1016/j.scitotenv.2008.12.017>.
- Wyn, B., Kidd, K.A., Burgess, N.M., Curry, R.A., Munkittrick, K.R., 2010. Increasing mercury in yellow perch at a hotspot in Atlantic Canada, Kejimikujik National Park. *Environ. Sci. Technol.* 44:9176–9181. <https://doi.org/10.1021/es1018114>.
- Xiao, Z.F., Strömberg, D., Lindqvist, O., 1995. Influence of humic substances on photolysis of divalent mercury in aqueous solution. *Water Air Soil Pollut.* 80:789–798. <https://doi.org/10.1007/BF01189730>.